Contributed paper for the Symposium "10 Years of Uranium Beam", April 2-4, 1986, GSI Darmstadt, W. Germany.

-3

Disk #34"Rehm2"

NUCLEAR STRUCTURE IN DEEP-INELASTIC REACTIONS

K. E. Rehm
Argonne National Laboratory, Argonne, IL 60439

CONF-8604184--3

DE86 014581

I. INTRODUCTION

About 10 years ago the first experiments with uranium beams were performed here at the GSI. One of these experiments[1] studied the reaction channels in the collision of two U-ions via direct particle detection. While this experiment failed to produce one of the "super-heavy nuclei" which at that time were predicted to have long half lives, it was one of the first experiments showing that heavy ion-reactions are more than just the collision of two liquid drops. Nuclear structure effects are clearly visible in a system involving the interaction of many nucleons. Since these first experiments, a large amount of new information has been gathered about the reaction mechanisms of heavy ion collisions. New processes have been observed like quasi-fission, incomplete fusion.., theoretical models have been developed which can describe individual aspects of the different reaction processes. From more detailed high resolution experiments, however, the picture emerged that the different reaction channels are correlated and influence each other. Through these correlations, nuclear structure effects can be seen even in complex collisions, which involve many nucleons and considerable energy transfers. Before the U + U experiment mentioned above, the exchange of nucleons between the two colliding nuclei was thought to be independent of the structure of the nuclei ("universal curve"[2]). The U + U results and also studies in many other systems[3,4] proved that this is not the case. The effects of nuclear shell structure are clearly visible. It was also found that these nuclear structure effects are mainly associated with processes during the entrance phase of the collisions. These early phases in the interaction of two nuclei, therefore, need some special attention, if one wants to study nuclear structure effects in deep inelastic collisions. I do not intend to give a review of all cases where fingerprints of nuclear structure effects have been observed in deep inelastic reaction studies, but rather concentrate on some recent experiments which were performed at Argonne. The results of the experiments indicate that the complicated deep inelastic reactions, which are usually described by

various statistical models evolve gradually from simple transfer processes, which have been studied extensively with lighter heavy ions like e.g. ^{16}O. Since no theory exists which connects the one-step DWBA theory on one side and the statistical models for multistep reactions on the other, I shall try as a first approach to describe this transition between quasi-elastic and deep inelastic reactions within a simple random walk model. In the last part of my contribution, I shall show some typical examples of nuclear structure effects.

II. EXPERIMENTAL RESULTS

After the first generation of deep inelastic reaction studies performed without individual mass and Z-resolution, the next generation of experiments has to deal with a detailed study of the contributions from individual reaction channels. This requires a detection system capable of resolving individual elements and isotopes in the outgoing channel with good efficiency. One of the experimental tools available in this field which has a large dynamic range, good resolution in particle detection, and also a resonably large solid angle is a magnetic spectrograph. As shown in several experiments[5] here at GSI spectrographs can resolve individual masses and charges up to about Xe.

At Argonne we have been limited so far to projectiles with masses up to A ≈ 80, and therefore the results I am going to present were obtained with medium mass ions. The energy was chosen to be in the vicinity of the Coulomb barrier. This has the advantage that the relative contributions from the quasi-elastic reactions which are important in the entrance phase are larger than at higher incident energies. Furthermore, the processes occur at lower velocities, with smaller angular momenta and effects of particle evaporation in the exit channels are of lesser importance. But even with these relatively light projectiles deep inelastic processes occur as can be seen from Fig. 1 where energy spectra for the system $^{48}Ti + ^{208}Pb$ at different scattering angles are shown.[6] The incident energy was about 25% above the Coulomb barrier for this system. The data were taken with the Enge Split Pole Spectrograph which due to its low dispersion covers the total energy range from quasi-elastic to deep-inelastic collisions with one magnetic field setting. The objective of this experiment was to measure the

contributions from individual channels to either quasi-elastic or deep inelastic collisions and to investigate if these two processes which can be easily separated at foward angles (see Fig. 1) are two distinct processes or evolve gradually from one to the other. With the good channel resolution which can be obtained from the ionization chamber in the focal plane of the spectrograph we are able to generate Wilczynski plots for individual transfer reactions in order to obtain answers to the question raised above. Results for some reaction channels are shown in Fig. 2.

Common to all channels which are shown in Fig. 2 is a broad ridge that extents increasingly towards forward angles as the Q-value becomes more negative (deep-inelastic orbiting component). The structure of this distribution is in good agreement with macroscopic calculations performed with the program of H. Feldmeier.[7] It should be noted that the outgoing particles are secondary reaction products and no corrections for particle evaporation effects have been applied. Calculations with the code PACE indicate that these corrections play a role mainly for large negative Q-values ($Q < -50$ MeV), i.e. in the region of the orbiting component where no large difference between the different reaction channels are observed. In addition to the broad orbiting component there is a steep mountain ridge associated with small Q-values (quasi-elastic component) and a maximum at a scattering angle $\theta_{cm} \approx 70°$. In all cases where both components are present, there is a gradual transition between the two processes. The minimum between

FIG. 1. Energy spectra from the reaction $^{48}Ti+^{208}Pb$ at different scattering angles.

FIG. 2. Wilczynski plots for several transfer reactions induced by ^{48}Ti on ^{208}Pb and E_{lab} = 300 MeV. The outermost solid contour line corresponds to a cross section of 0.01 mb/(rad MeV) with an increase by a factor of 10 for each subsequent line. The dashed lines correspond to cross sections of 2 or 5 times the values for the solid lines.

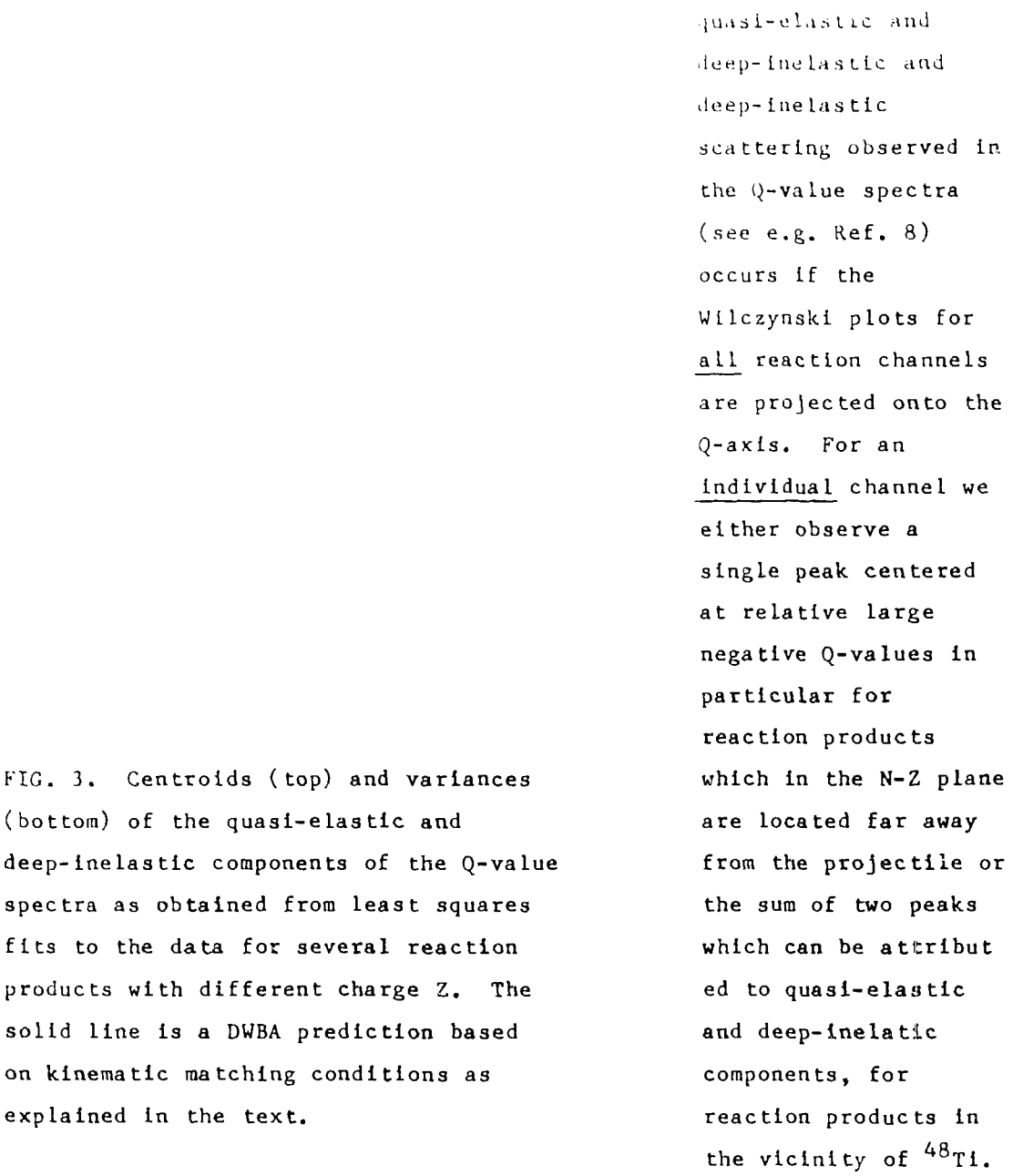

FIG. 3. Centroids (top) and variances (bottom) of the quasi-elastic and deep-inelastic components of the Q-value spectra as obtained from least squares fits to the data for several reaction products with different charge Z. The solid line is a DWBA prediction based on kinematic matching conditions as explained in the text.

quasi-elastic and deep-inelastic and deep-inelastic scattering observed in the Q-value spectra (see e.g. Ref. 8) occurs if the Wilczynski plots for all reaction channels are projected onto the Q-axis. For an individual channel we either observe a single peak centered at relative large negative Q-values in particular for reaction products which in the N-Z plane are located far away from the projectile or the sum of two peaks which can be attributed to quasi-elastic and deep-inelatic components, for reaction products in the vicinity of ^{48}Ti.

The centroids of these two distributions approximated by two Gaussions are shown in Fig. 3a for several elements produced in the collision of $^{48}Ti + {}^{208}Pb$. Generally the centroids move to more negative Q-values the further the reaction product is away from Z=22 (Ti). The centroid of the quasi-elastic component which is observed for reaction products between Ti(Z=22) and K(Z=19) follows closely the line expected from optium Q-value calculations performed with the code PTOLEMY.[9] Parallel to this quasi-elastic Q-value distribution there is a second peak centered at about 25 MeV more negative Q-values associated

with deep inelastic reactions. The widths of there distributions decrease as the charge transferred during the interaction increases (see Fig. 3b). Similar results were obtained for reactions induced by Ni ions.[10]

The behavior of the cross sections reflected in the individual Wilczynski plots suggests that the deep-inelastic processes can be interpreted as multistep transfer reactions which occur at more and more negative Q-values the more interaction steps are involved. These processes evolve gradually from simple quasi-elastic transfer reactions [in particular (^{48}Ti, ^{49}Ti) and (^{48}Ti, ^{47}Sc)] to collisions which last long enough to allow multiple particle transfer but involve large enough angular momenta so that compound nucleus formation is not possible.

FIG. 4. Schematic transfer routes for the population of multi-particle-multi-hole states in reactions between heavy ions (see text for details.

A schematic picture for such a process is shown in Fig. 4. A one-step proton transfer starting from ^{48}Ti + ^{208}Pb can lead to the population of (Q-matched) states in ^{47}Sc + ^{209}Bi at small excitation energies. If for a more central collision the interaction time is long enough to allow a second transfer step, either states in the system ^{46}Ca + ^{210}Po can be populated or the second step can lead back to ^{48}Ti + ^{208}Pb, but not necessarily to the ground state. As known from light ion induced reactions (e.g. ^{209}Bi(d,^{3}He)^{208}Pb) mainly 1p-1h states in

^{208}Pb at ~5 MeV excitation energy are populated in this proton pickup reaction.[11] For even longer interaction times, multistep reactions can populate successively more complicated np-nh states in the neighborhood of ^{48}Ti and ^{208}Pb. For neutron transfer similar considerations apply.

A microscopic description of these multistep processes has not been performed so far. One nucleon transfer reactions induced by heavy ions are usually well understood within one-step DWBA calculations.[12] But already a two proton transfer reaction like (^{16}O, ^{14}C) is underpredicted in DWBA by factors of 100-1000, even including successive transfers.[13] There is a real need for a better theoretical understanding for these processes which are not yet of statistical nature, but are already too complicated for simple DWBA calculations.

In order to get a first idea about the principles underlying the exchange of nucleons in these multistep reactions we have performed random walk calculations on a two dimensional N-Z-lattice. If each displacement vector on this lattice is described by (0,1), (1,0) (0,-1), (-1,0) including inelastic scattering with (0,0), then the probability distribution $P_n(N,Z)$ after n steps is given by the equation

$$P_n(N,Z) = Q_n \sum_{i=0}^{4} P_{n-1}[(N,Z)-\Delta_i]\cdot T_i[(N,Z) - \Delta_i] \qquad (1)$$

where $T_i[(N,Z) - \Delta_i]$ are the properly normalized transtion probabilities from the position $[(N,Z) - \Delta_i] \rightarrow (N,Z)$ and Q_n is the probability that a transfer reaction involving n-steps occured, which was calculated within a perturbative statistical model developed by Tanabe.[14] In the calculations with equation (1) different transition probabilities T_i for the different reaction steps n can be used. It can thus be investigated if the entrance phase is governed by Q-matching effects and to what extent in later stages a stochastic exchange of protons and neutrons occurs. Furthermore, complicated non-analytic driving potentials can easily be incorporated in a random walk calculation. Therefore effects of shell corrections on the direction of the mass flow for nuclei in the vicinity of closed shells can be studied in detail. Several random walk descriptions have been published in the literature (15-17). The effect that each step has to be weighted by Q_n, however, has been generally

neglected.

Within this model we have calculated the production cross sections and Q-value spectra for several reaction channels near ^{48}Ti. The cross section for all transfer channels was fixed to 1000 mb and the energy loss per transfer step was taken from Ref. 18.

The best agreement with the experimental data is obtained if we assume that the transition probabilities in the first step are determined by direct-reaction Q-matching, whereas from step 2 on a random exchange of protons and neutrons in both directions occurs. The results for the integrated cross sections and the mean Q-values are shown in Fig. 5, while results for the Q-value spectra for different reaction channels are given in Fig. 6. Taking into account that all parameters (energy loss per transfer step, probability for the occurrence of n step reactions, driving potential) were taken from the literature, the agreement between the simple model and the data is quite satisfactory. Some results for the systems ^{58}Ni and ^{64}Ni + ^{208}Pb calculated under the same assumption as in the ^{48}Ti + ^{208}Pb system, are shown in Fig. 7. It can be seen that the direction of the charge flow in the two cases which favors the production of reaction products with

FIG. 5. Comparison of experimental data and theoretical predictions for integrated cross sections and average Q-values for several reaction channels from the reaction ^{48}Ti + ^{208}Pb at E_{lab} = 300 MeV.

FIG. 6. Measured Q-value spectra (histograms) and theoretical predications (solid lines) for several reaction channels from the interaction of $^{48}Ti + ^{208}Pb$ at $E_{lab} = 300$ MeV.

$Z < 27$ for the system $^{58}Ni + ^{208}Pb$ is reproduced in the calculations. The asymmetry in the charge flow in the case of $^{58}Ni + ^{208}Pb$ has its origin in kinematic matching conditions as does the asymmetry in the charge transfer for the system $^{16}O + ^{208}Pb$. Q-matching considerations, therefore, play an important role in the entrance phase of the reaction as observed also for reactions induced by lighter projectiles. For our system they produce in some cases a shift of the centroids of the charge and mass distributions towards lower Z and larger N. This shift has only recently been observed, when experiments with sufficient resolutions were performed.[5] Starting with the second or third step, however, the interaction of the two nuclei is already so strong that the driving potential (which is usually calculated under the assumption of

two separate spheres) is of minor importance and neutrons and protons are exchanged with equal probability.

III. NUCLEAR STRUCTURE EFFECTS

Nuclear structure effects have been observed in several systems mainly in the early reaction phase. As already mentioned in the introduction U + U was one of the first examples.[1] There are several experiments[3,4] showing that the energy necessary to exchange a proton is different for nuclei near closed shells if compared to systems which are away from shell closures. This effect lead Dakowski et al. to introduce a structure dependent energy loss term.[3]

Another example of nuclear structure effects in deep inelastic collisions has been observed in the direction of the mass flow measured in the reactions $^{144}Sm + ^{144}Sm$ and $^{154}Sm + ^{154}Sm$. The ^{144}Sm nucleus is located on the closed N=82 shell and therefore a larger proton exchange rate is observed for $^{144}Sm + ^{144}Sm$ as compared to $^{154}Sm + ^{154}Sm$ (Ref. 19). Calculations within the random walk model[17] are able to reproduce these differences for the two systems.

FIG. 7. Comparison of experimental data and theoretical predictions for integrated cross sections from the systems $^{58}Ni + ^{208}Pb$ $^{64}Ni + ^{208}Pb$.

Effects of nuclear structure have been observed more recently in the way the excitation energy is shared between the two reaction partners. While in earlier measurements[20] it was deduced that the excitation energy is shared in proportion to the mass of the interacting nuclei, experiments for the system $^{86}Kr + ^{208}Pb$ have shown that the situation is more complicated.[21] In particular, in the entrance phase of interaction a large fraction of the excitation energy goes into the lighter partner if a neutron pickup reaction (e.g. ^{86}Kr, ^{87}Kr) occurs. In a neutron stripping reaction on the other hand, the residual nucleus obtains a larger fraction of the excitation energy. Similar observations have been made for ^{16}O and ^{18}O induced reactions (see e.g. Ref. 22).

Other examples of nuclear structure effects were found in experiments with ^{238}U beams on Sn and Pd targets where correlated proton transfer processes have been observed. Details about these experiments will be given in the contribution by H. J. Körner.[23]

As a final example for nuclear structure effects, I want to discuss the influence of the neutron number on the strength of quasi-elastic and deep-inelastic collisions. As mentioned in section II there is no clear distinction between the two processes. Deep inelastic collisions evolve gradually from the quasi-elastic processes. In order to extract cross section for the two reaction types from the experimental data, two different procedures can be used. One involves the parameterization of the angular distribution into a gaussian (quasi-elastic) and exponential (deep-inelastic) component. The other methods uses an (arbitrary) cut in the Q-value spectra. Based on the structure of the Wilczynski plots shown in Fig. 2 Q = -30 MeV was chosen for this value. Events with $Q > -30$ MeV are attributed to quasi-elastic processes while events with $Q < -30$ MeV are ascribed to deep-inelastic reactions. All systems were treated by the same procedure. In Fig. 8, I have plotted the relative contributions of quasi-elastic and deep inelastic reactions to the total transfer cross section measured for the systems $^{46,48,50}Ti$ and $^{58,64}Ni + ^{208}Pb$ as function of the neutron number in the projectile. There is a clear decrease of the strength of quasi-elastic reactions with increasing neutron number at the expense of more complicated multistep reactions associated with larger negative Q-values. While for $^{46}Ti +$

FIG. 8. Relative contributions of quasi-elastic and deep-inelastic processes to the total transfer cross sections as function of the neutron number in the projectile as measured in the systems $^{46,48,50}Ti + ^{208}Pb$ and $^{58,64}Ni + ^{208}Pb$.

^{208}Pb there are about equal amounts of quasi-elastic and deep inelastic scattering this ratio changes to about 2:1 in favor of the deep-inelastic reactions for $^{64}Ni + ^{208}Pb$. Similar results have been obtained for $^{58,64}Ni + ^{112-124}Sn$.

The differences between neutron rich and neutron deficient projectiles become even stronger if one lowers the bombarding energy. In Fig. 9 are plotted the cross sections for processes which are not associated with peripheral quasi-elastic collisions, i.e. the sum of

FIG. 9. Energy dependence of the sum of the cross sections for deep-inelastic, quasi-fission and fusion-fission processes as measured in the systems $^{58}Ni + ^{208}Pb$ (circles) and $^{64}Ni + ^{208}Pb$ (triangles).

deep-inelastic, fusion and quasi-fission events measured for the system $^{58,64}Ni + ^{208}Pb$ as function of the incident energy. It is clear from Fig. 9 that at lower energies the system $^{64}Ni + ^{208}Pb$ shows larger cross sections (by about a factor of 2) for these non-peripheral collisions as compared to the system $^{58}Ni + ^{208}Pb$. The reason for this difference between the systems $^{58}Ni + ^{208}Pb$ and $^{64}Ni + ^{208}Pb$ is not yet clear. In this context is should be mentioned that similar differences were observed for the fusion cross sections in the systems $^{58}Ni + ^{64}Ni$ and $^{58}Ni + ^{58}Ni$ (Ref. 24). This experiment also still lacks a thorough theoretical explanation.

IV. SUMMARY

The study of deep-inelastic collisions has now gone into a stage where more and more high resolution data become available. From the data it becomes clear that the two colliding nuclei can not be considered as two drops of nuclear matter. In particular, in early stages of the collision nuclear structure effects can influence the development of the reaction, and even for large energy losses, corresponding to longer interaction times, these structure effects are still visible as seen e.g. in the behavior of charge variances for large negative Q-values.[3] These early reaction stages are not understood theoretically. Multistep DWBA calculations are still orders of magnitude away from a satisfactory description of these processes. As shown for the system $^{58,64}Ni + ^{208}Pb$ there are similarities between these heavy systems and anomalies found in lighter nuclei. Thus, a better understanding of deep inelastic reactions might also influence the development in other fields of heavy ion research.

The experiments at Argonne were performed in collaboration with A. van den Berg, J. Kolata (Notre Dame), D. Kovar, W. Kutschera, L. L. Lee (SUNY), G. Rosner, G. Stephans, R. Vojtech (Notre Dame) and J. Yntema.

This research was supported by the U. S. Department of Energy, Nuclear Physics Division, under Contract W-31-109-Eng-38.

References

[1]K. D. Hildenbrand et al., Phys. Rev. Lett. 39, 1065 (1977).

[2]J. R. Huizenga et al., Phys. Rev. Lett. 37, 885 (1976).

[3]M. Dakowski et al., Nucl. Phys. A378, 189 (1982).

[4]K. E. Rehm et al., Nucl. Phys. A366, 411 (1981).

[5]D. Schüll et al., Nucl. Letts. 102B, 116 (1981).

[6]K. E. Rehm et al., Suppl. Journal Phys. Soc. Japan 54, 410 (1985).

[7]H. Feldmeier: Dynamics of Heavy Ion Reactions; in Nuclear Structure and Heavy Ion Dynamics, ed. L. Moretto and R. A. Ricci, North Holland 1984.

[8]H. J. Wollersheim et al., Phys. Rev. C24, 2114 (1981).

[9]M. H. MacFarlane and S. C. Pieper, Argonne National Laboratory Report No. ANL-76-11 (Rev. 1), 1978.

[10]K. E. Rehm et al., to be published.

[11]E. A. McClatchie et al., Phys. Rev. C1, 1828 (1970).

[12]S. C. Pieper et al., Phys. Rev. C18, 180 (1978).

[13]P. P. Tung et al., Phys. Rev. C18, 1663 (1978).

[14]H. Tanabe, Nucl. Phys. A423, 139 (1984).

[15]J. J. Griffin et al., Nucl. Phys. A369, 184 (1981).

[16]D. Bangert et al., GSI Annual Report 1982 and to be published.

[17]J. Töke and A. Gobbi, GSI Scientific Report 1981, p. 91.

[18]T. Mikumo et al., Phys. Rev. C21, 620 (1981).

[19]K. D. Hildenbrand et al., Nucl. Phys. A405, 179 (1983).

[20]C. R. Gould et al., Z. Phys. A284, 353 (1978) and Z. Phys. A294, 323 (1980).

[21]H. Sohlbach et al., Phys. Lett. 153B, 386 (1985).

[22]H. Spieler et al., Z. Phys. A278, 241 (1976).

[23]H. J. Körner, contribution to this symposium.

[24]M. Beckerman et al., Phys. Rev. Lett. 45, 1472 (1980).

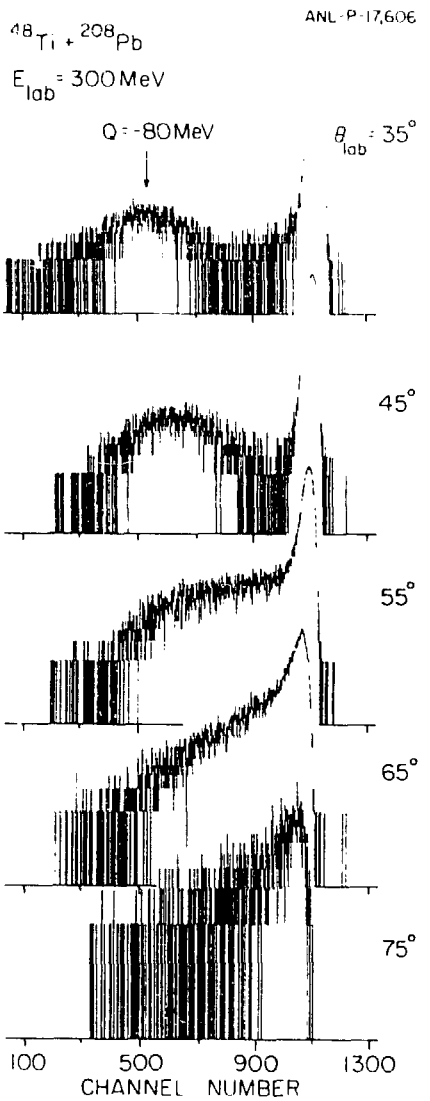
ANL-P-17,606
$^{48}Ti + ^{208}Pb$
E_{lab} = 300 MeV
Q = -80 MeV
θ_{lab} = 35°
45°
55°
65°
75°
100
500
900
1300
CHANNEL NUMBER

Fig. 1

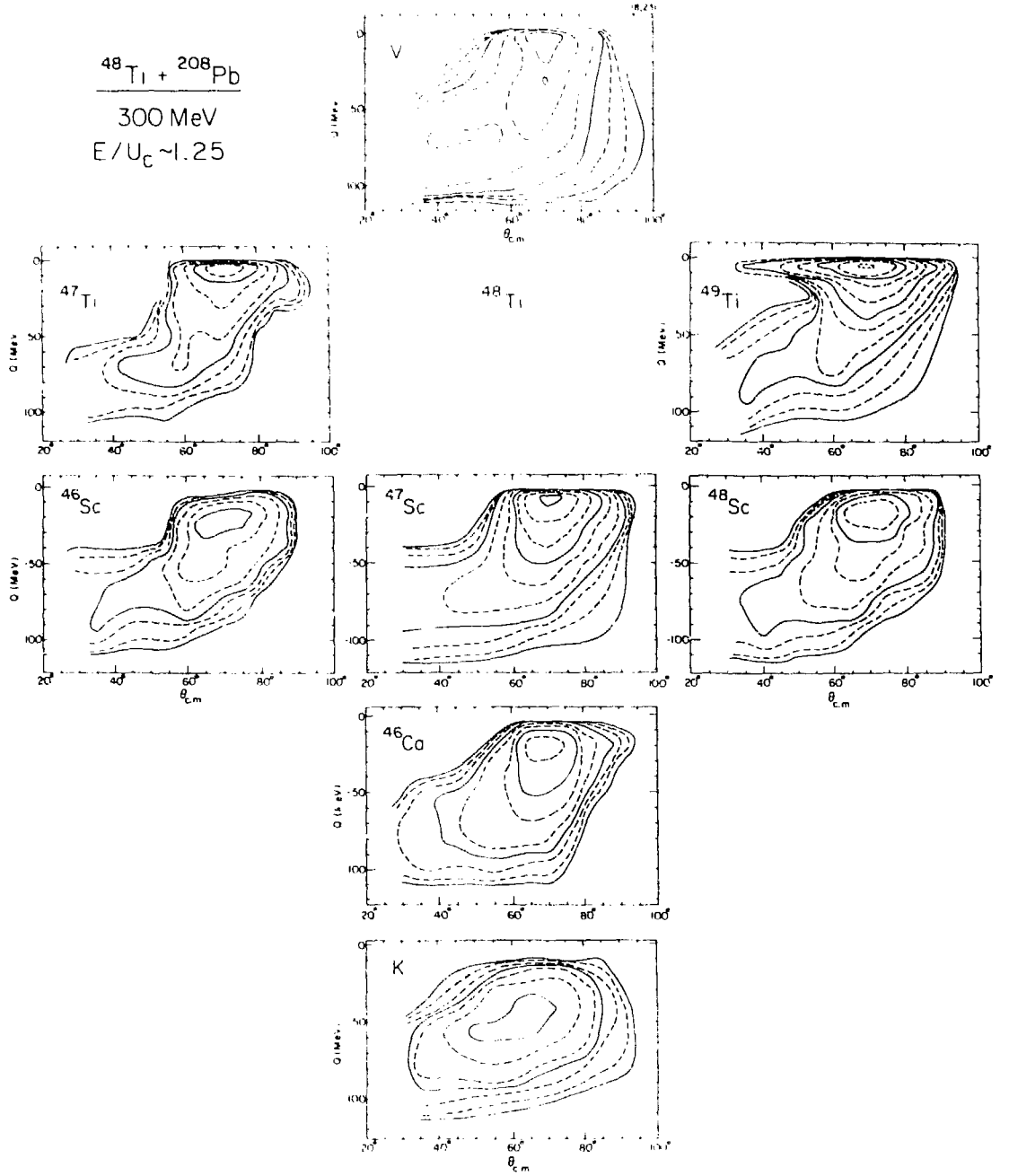
48Ti + 208Pb
300 MeV
E/Uc ~1.25
V
47Ti
48Ti
49Ti
46Sc
47Sc
48Sc
46Ca
K
Q (MeV)
θc.m

Fig. 2

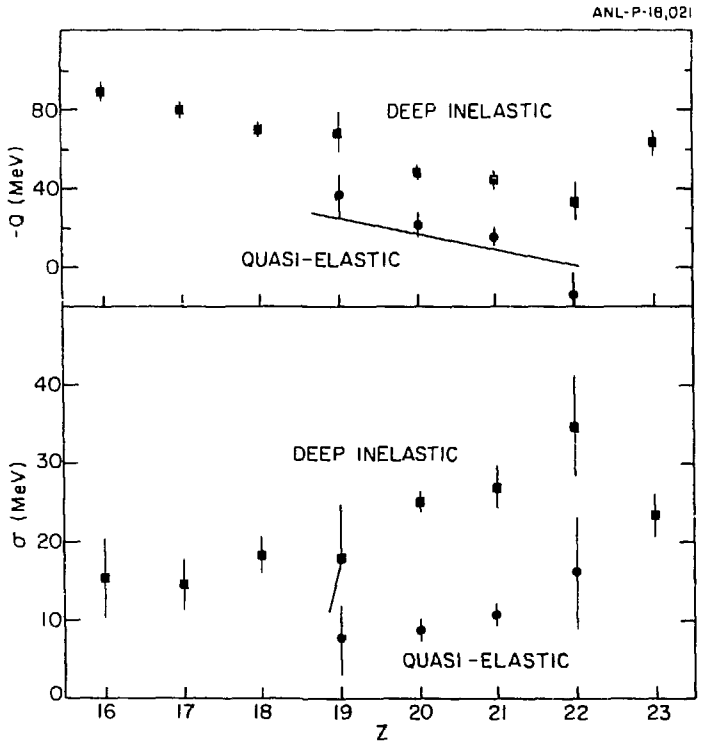
ANL-P-18,021
DEEP INELASTIC
QUASI-ELASTIC
-Q (MeV)
80
40
0
DEEP INELASTIC
QUASI-ELASTIC
σ (MeV)
40
30
20
10
0
16
17
18
19
20
21
22
23
Z

Fig. 3

ANL-P-18,026

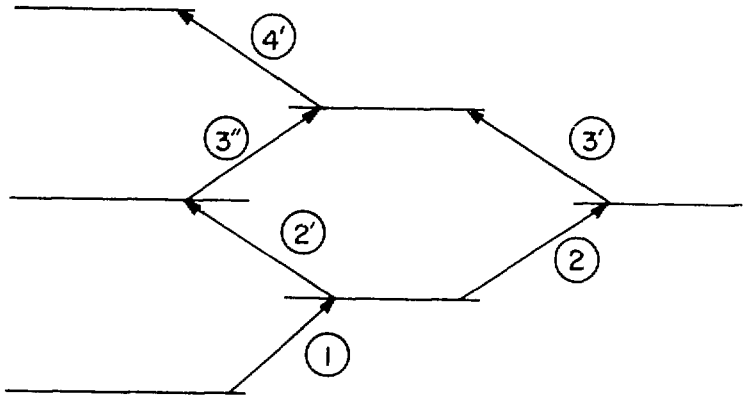

A	A + 1	A + 2
^{208}Pb	^{209}Bi	^{210}Po
+	+	+
^{48}Ti	^{47}Sc	^{46}Ca

Fig. 4

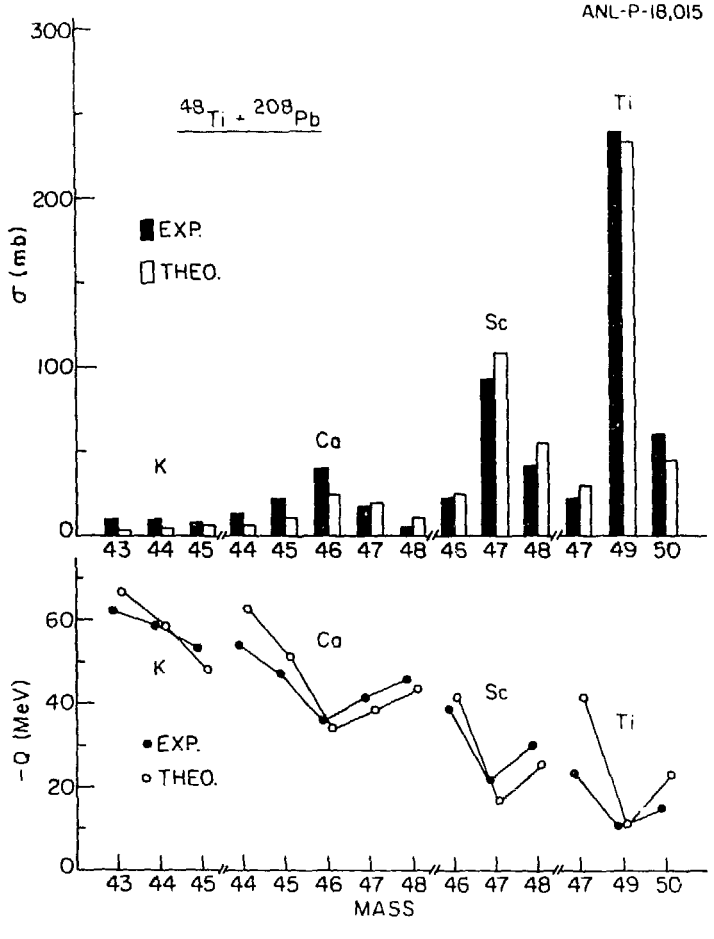
ANL-P-18,015
$^{48}Ti + ^{208}Pb$
EXP.
THEO.
σ (mb)
300
200
100
0
K
Ca
Sc
Ti
43 44 45 44 45 46 47 48 46 47 48 47 49 50
-Q (MeV)
60
40
20
0
K
Ca
Sc
Ti
EXP.
THEO.
43 44 45 44 45 46 47 48 46 47 48 47 49 50
MASS

Fig. 5

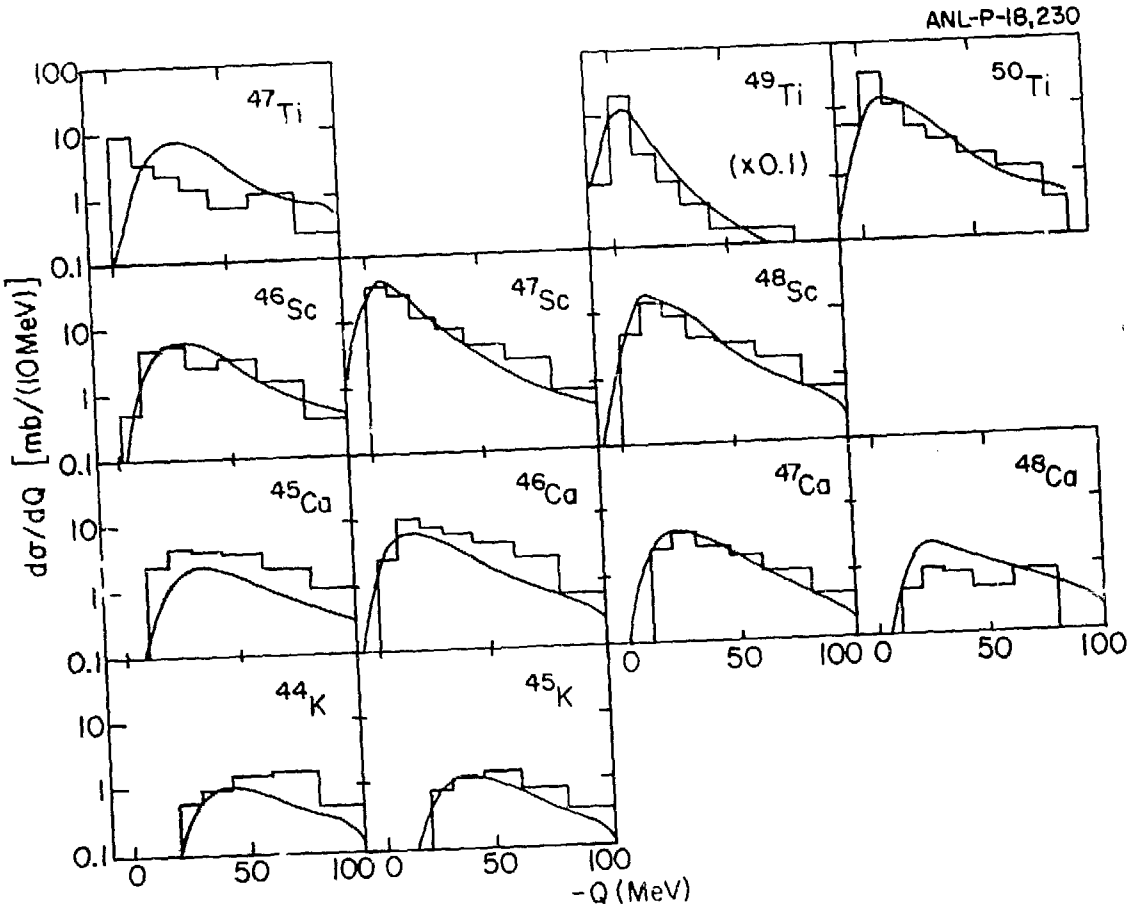
ANL-P-18,230
^{47}Ti
^{49}Ti
(x0.1)
^{50}Ti
^{46}Sc
^{47}Sc
^{48}Sc
^{45}Ca
^{46}Ca
^{47}Ca
^{48}Ca
^{44}K
^{45}K
dσ/dQ [mb/(10MeV)]
-Q (MeV)
100
10
1
0.1
0
50
100

Fig. 6

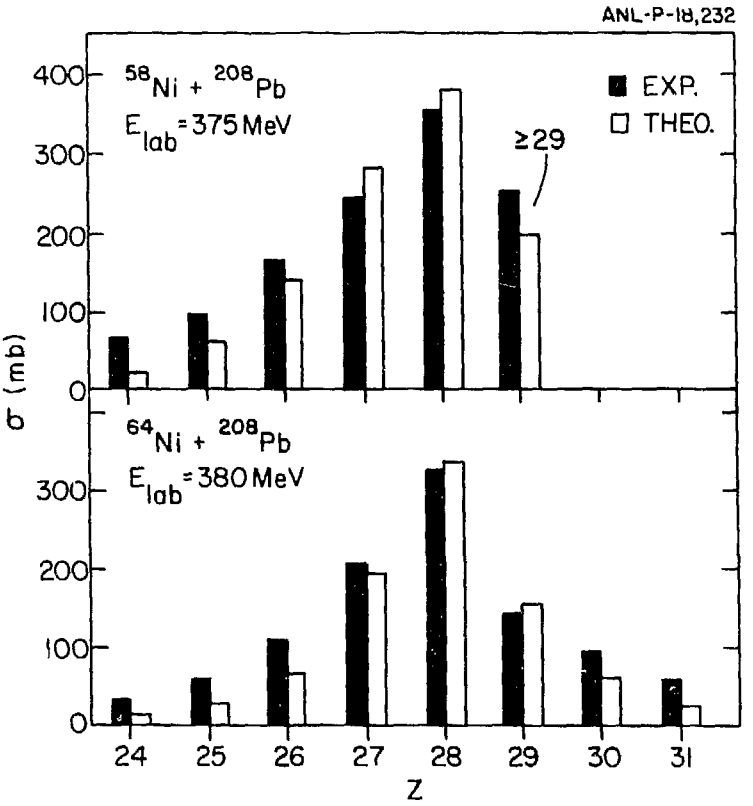
ANL-P-18,232
$^{58}Ni + ^{208}Pb$
E_{lab} = 375 MeV
EXP.
THEO.
≥29
$^{64}Ni + ^{208}Pb$
E_{lab} = 380 MeV
σ (mb)
400
300
200
100
0
24
25
26
27
28
29
30
31
Z

Fig. 7

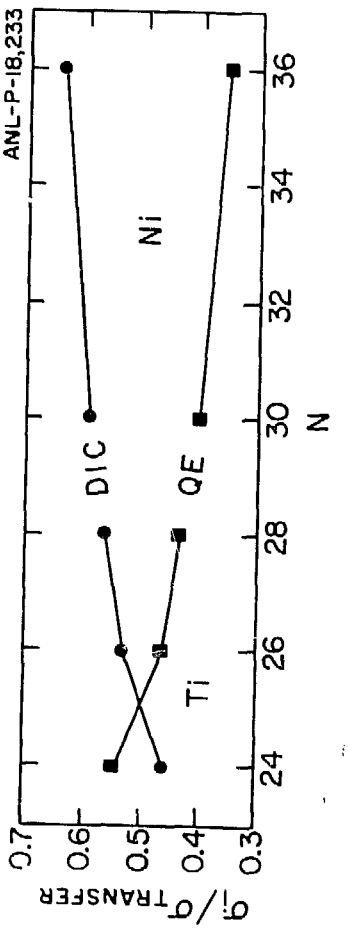
ANL-P-18,233
Ni
Ti
DIC
QE
N
$q_i/q_{TRANSFER}$
0.7
0.6
0.5
0.4
0.3
24
26
28
30
32
34
36

Fig. 8

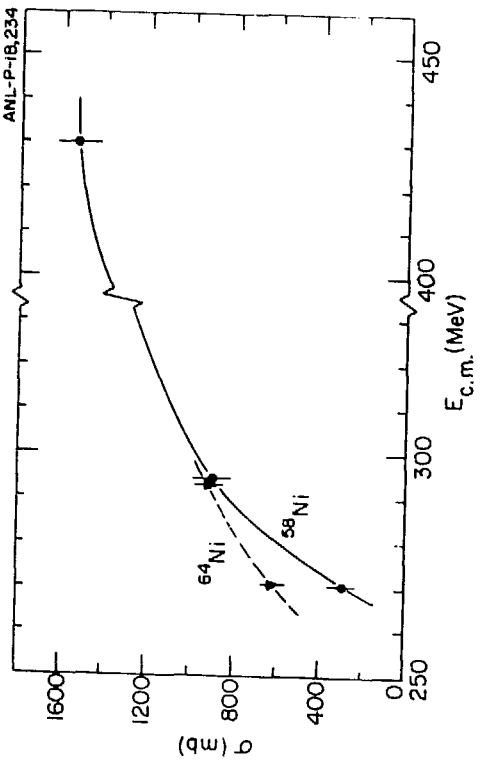
ANL-P-18,234
σ (mb)
1600
1200
800
400
0
250
300
400
450
$E_{c.m.}$ (MeV)
^{64}Ni
^{58}Ni

Fig. 9

DISCLAIMER